

# Koopman Model Dimension Reduction via Variational Bayesian Inference and Graph Search

Selin Ezgi Özcan<sup>a,\*</sup>, Mustafa Mert Ankaralı<sup>b</sup>

<sup>a</sup>*Department of Electrical Sustainable Energy, Delft University of Technology, Delft, The Netherlands*

<sup>b</sup>*Department of Electrical and Electronics Engineering, Middle East Technical University, Ankara, Turkey*

---

## Abstract

Koopman operator recently gained increasing attention in the control systems community for its abilities to bridge linear and nonlinear systems. Data driven Koopman operator approximations have established themselves as key enablers for system identification and model predictive control. Nonetheless, such methods commonly entail a preselected definition of states in the function space leading to high dimensional overfitting models and degraded long term prediction performances. We address this problem by proposing a hierarchical probabilistic approach for the Koopman model identification problem. In our method, elements of the model are treated as random variables and the posterior estimates are found using variational Bayesian (VB) inference updates. Our model distinguishes from others in the integration of inclusion flags. By the help of the inclusion flags, we intuitively threshold the probability of each state in the model. We then propose a graph search based algorithm to reduce the preselected states of the Koopman model. We demonstrate that our reduction method overcomes numerical instabilities and the reduced models maintain performance in simulated and real experiments.

*Keywords:* System identification, Koopman operator, Variational Bayesian inference, Graph theory

---

## 1. Introduction

In recent years, Koopman operator has attracted significant attention in various fields of control systems due to its ability to represent nonlinear dynamical systems with globally linear models [1]. Rather than linearizing the system around specific operating points in the state space, the Koopman approach introduces exact linear models in the function space [2]. The dynamics in the function space is linear, so the operator enables the use of a vast amount of well established linear systems tools on nonlinear systems, significantly improving the workflow. Despite its promise, the Koopman operator is inherently infinite dimensional and not directly applicable in real world settings. Therefore, finite dimensional approximations of the operator is needed for practical implementation [3].

Pioneering works have fostered the adoption of the data driven finite dimensional approximation of

the Koopman operator particularly in system identification and model based control [4, 5, 6, 7]. These methods approximate the operator on a finite dimensional subspace which is spanned by an a priori selected dictionary of functions. It is common in the literature to denote the functions in the dictionary as observables. Based on the values of the observables on the measured dataset, linear regression is performed to estimate the Koopman operator as a matrix [4, 5]. The eigenspace of this matrix then provides detailed and interpretable information about the system behavior, which has proven to be valuable in a wide range of system identification and control applications [3].

Existing data driven approximation methods, however, typically lack a structured and principled workflow for model construction. The a priori selected dictionary plays a major role in the description and prediction quality of the model [8, 9, 10]. If the dictionary adequately captures the dominant nonlinearities and yields numerically well conditioned optimization problems, the resulting Koopman model can exhibit strong generaliza-

---

\*Corresponding author.

Email addresses: [seozcan@tudelft.nl](mailto:seozcan@tudelft.nl) (Selin Ezgi Özcan), [mertan@metu.edu.tr](mailto:mertan@metu.edu.tr) (Mustafa Mert Ankaralı)

tion performance. Yet, the selection of an appropriate dictionary is highly system dependent and no universal choice exists [8]. Some approaches rely on encoder-decoder architectures to implicitly learn the dictionary [10]. Deep learning solutions [11] usually can learn the embeddings well, but the deep models may not be as easily interpretable as standard approaches. Often, deep learning based approaches need dedicated hardware and large amounts of data [12]. This prioritizes more conventional methods whenever possible. Traditional Koopman approximation methods commonly use predetermined polynomial bases, radial basis functions (RBF), particularly squared exponential kernels and Fourier features in the dictionary [3]. Even when a particular class of observables is selected for the dictionary, the parameters related to the functions remain unspecified. For example, the exponent coefficient of squared exponential kernels or polynomial degree must also be determined. Moreover, the chosen observables may cause ill conditioned problems since observables are nonlinear functions of the measured states, measurement noise is transformed in a nontrivial and generally unknown manner. As a result, the noise characteristics of the observables cannot be quantified a priori and the nonlinear mapping may significantly amplify or distort the noise, thereby degrading numerical conditioning [13]. Another open design question is the size of the dictionary. In principle, the span of the dictionary must be invariant under the operator. However, this is almost never realizable in the finite dimensional setting for practical scenarios. In the finite dimensional setting, this requirement corresponds to ensuring that the projection of the finite dimensional operator's image onto the chosen dictionary incurs only a small approximation error [3]. Adding more observables does not necessarily reduce the approximation error, and may even exacerbate prediction errors [8].

These open problems reveal the need for systematic assessment of the dictionary and informed observable selection. [14] selects the regression variables by sequential thresholded least squares approach, where observables are pruned based on the magnitudes of their weights. This approach treats each target variable independently, without providing guidance for dictionary selection when multiple target variables are considered. Furthermore, it does not account for how differences in the scaling of observables affect the resulting weights. Moreover, setting a single threshold for various types of

observables is not very meaningful in the physical sense as each observable and state may have different physical units. Another work [8] highlights the misleading performance of the one step prediction error metric as the objective for the Koopman model problems and demonstrates that some Koopman models can perform reasonably well in one step prediction but they actually fail to do prediction in long term, which is crucial for model predictive control. They assign an inclusion variable to each dictionary element and set them as hyperparameters to a control related cost function, which they optimize using tree structured Parzen estimators [15].

In our work, we propose a hierarchical probabilistic model for the Koopman model identification problem. As opposed to the deterministic treatments of unknown variables, the probabilistic approach models unknowns as random variables and estimates the parameters of the density function. Our hierarchy includes inclusion variables modeled as Bernoulli random variables as well as uncertainty estimates of parameters. Maximum a posteriori (MAP) estimation via variational Bayesian (VB) inference is performed to get the estimates of all random variables. The inclusion variables correspond to the existence probabilities of the dictionary elements, they provide scale free and probabilistic thresholding metrics as a natural byproduct. By thresholding the expectation of this random variable, we flag each dictionary element as either included or discarded. We build a matrix of these flags that represent a directed graph with the dictionary elements as vertices. By graph condensation and ancestry search, we find a subset of the initial dictionary of observables that affect the output states of the Koopman model. A similar work [16] has explored hierarchical inference techniques in identifying nonlinearities without the Koopman operator context. The work consequently did not require graph based dictionary reduction because a state space approach is not considered. Another work [17] focused on exploring the subsystems in a dynamical model using a graph theory perspective, but the scope is not tailored to immediately apply to the Koopman models. In this work, we bridge this gap and step by step detail how a Koopman model can naturally be interpreted as a graph and demonstrate how dictionary reduction is possible.

Our contributions in this paper are listed as:

- We provide hierarchical probabilistic modeling of the Koopman problem. Our formulation dis-

tinguishes weight magnitudes from inclusion in the model.

- We derive the VB inference updates for our proposed model.
- By resorting to graph techniques, we reduce the Koopman model size in a way that the output variables remain unaffected by the reduction.
- We show that other traditional tools for Koopman model identification also benefit from the reduced dictionary after our proposed algorithm is applied.
- We demonstrate the performance of our methods in both simulated and real world settings.

This paper is organized as follows. In Section 2, we provide the preliminaries about the Koopman operator, VB inference and basic graph condensation. Section 3 outlines the problem and introduces the probabilistic model which we propose. Then in Section 4, we derive the VB updates and provide our dictionary reduction algorithm based on the inclusion random variables. In Section 5, we demonstrate the results of our experiments. Lastly, a conclusion and discussion is given in Section 6.

## 2. Preliminaries

### 2.1. Koopman Operator and Data Driven Approximations

Let a discrete time dynamical system be described by the map  $\mathbf{S} : X \rightarrow X$ ,

$$\mathbf{x}[k+1] = \mathbf{S}(\mathbf{x}[k]), \quad (1)$$

where  $X$  is the state space of the system and  $k$  is the discrete time index [3]. In our context, we simply assume  $X \subset \mathbb{R}^d$ . An observable  $\psi \in \mathcal{H}$  is defined as a scalar valued function of the state  $\psi : X \rightarrow \mathbb{R}$ , where  $\mathcal{H}$  is a Hilbert space. Letting  $\mathcal{L}(\mathcal{H})$  be the operator space on  $\mathcal{H}$ , the discrete time Koopman operator  $\mathcal{K} \in \mathcal{L}(\mathcal{H})$  is defined through its action on the observables by the system specific composition [2]

$$\mathcal{K}\psi = \psi \circ \mathbf{S}. \quad (2)$$

The Koopman operator is linear in its arguments and thus provides a global linear representation for the system unlike linearization around a point in

the state space. However, the operator suffers from possible infinite dimensionality [3].

Data driven algorithms such as Extended Dynamic Mode Decomposition (EDMD) have been proposed to circumvent the infinite dimensionality problem [5]. EDMD aims to approximate the operator in a finite dimensional subspace spanned by a predefined set of observables and express the action of the operator as a matrix with a predefined set of observables as the basis [3, 5]. Let the dictionary of observables be  $\phi(\mathbf{x}) = [\phi_1(\mathbf{x}) \dots \phi_L(\mathbf{x})]^T$  and  $F \in \mathcal{H}$  be the subspace spanned by  $\phi$ . Since  $F$  is a finite dimensional subspace, the restriction of  $\mathcal{K}$  from and onto  $F$  can be represented as a matrix  $\mathbf{K}_F$  with the basis  $\phi$ . The aim of EDMD is to approximate  $\mathbf{K}_F$  as  $\hat{\mathbf{K}}_F$  through least squares solutions of the optimization problem [3, 5]:

$$\hat{\mathbf{K}}_F = \arg \min_{\mathbf{K}_F \in \mathbb{R}^{L \times L}} \sum_{i=1}^M (\phi(\mathbf{x}[i+1])^T - \phi(\mathbf{x}[i])^T \mathbf{K}_F)^2. \quad (3)$$

One of the most useful extensions of the algorithm adapts the approach for controlled systems while maintaining the basic workflow [6]. At the end, EDMD with control input models provide a linear state space structure in terms of the dictionary elements as the states:

$$\begin{aligned} \phi(\mathbf{x}[k+1])^T &= [\phi(\mathbf{x}[k])^T \mathbf{u}[k]^T]^T \hat{\mathbf{K}}_F \\ \mathbf{x}[k] &= \mathbf{C}\phi(\mathbf{x}[k]). \end{aligned} \quad (4)$$

### 2.2. Variational Bayesian (VB) Inference

The Koopman EDMD model identification is a classic least squares regression problem once the dictionary is set and data is collected [5, 18]. While the pseudo inverse solution is straightforward, the matrix approximation can perform poorly especially in highly noisy data sets due to ill conditioned matrices. On the other hand, probabilistic regression models can extract the desired information through the so called hidden variables and hyperparameters. In a probabilistic model with the observed data denoted as  $\mathbf{x}$ , the hidden variables  $\mathbf{z}$  are unobserved variables in the model with generating parameters  $\boldsymbol{\theta}$  and data generating probability density  $p(\mathbf{x}, \mathbf{z} | \boldsymbol{\theta})$  [13, 18].

VB inference provides an approximate Bayesian treatment of probabilistic models with hidden variables by replacing the posterior  $p(\mathbf{z} | \mathbf{x}, \boldsymbol{\theta})$  with a known parameterized distribution family  $q(\mathbf{z})$ . VB

then connects naturally to the Expectation Maximization (EM) algorithm [19] by maximizing the evidence lower bound

$$\mathcal{L}(q, \theta) = \int q(\mathbf{z}) \log \frac{p(\mathbf{x}, \mathbf{z} | \theta)}{q(\mathbf{z})} d\mathbf{z} \quad (5)$$

in an alternating manner in E and M steps [13, 18]. In particular, if the model lacks the generating parameters  $\theta$  and only contains hidden variables  $\mathbf{z}$ , then the VB inference executes only the E step [13].

In the presence of several hidden variables, the mean field approximation for the adopted distributions of the hidden variables can be implemented [20]:

$$q(\mathbf{z}) = \prod_{i=1}^N q_i(z_i), \quad (6)$$

where  $N$  is the number of hidden variables. Thus, the posterior distribution of each hidden variable is updated as [13]

$$\log q_i^*(z_i) = \mathbb{E}_{\mathbf{z}_{j \neq i}} [\log p(\mathbf{x}, \mathbf{z})] + \text{const.} \quad (7)$$

### 2.3. Condensation of a Graph

Given a directed graph  $G = (V, E)$  with the vertex set  $V$  and the edge set  $E$ , a strongly connected component (SCC) is defined as a subset  $S \in V$  where every  $u, v \in S$  are mutually reachable from another; i.e, directed paths exist between the two vertices in both directions. SCCs constitute maximal subgraphs that are internally reachable. Given a directed graph  $G$ , an associated condensed graph  $G_C$  can be constructed by letting each SCC be a node. The condensed graph  $G_C$  of  $G$  essentially captures the coarse interactions between these maximal subgraphs. Let  $\{S_i\}_{i=1}^{N_S}$  be the SCCs of  $G$ . We construct  $G_C = (V_C, E_C)$  as  $V_C = \cup_{i=1}^{N_S} \{S_i\}$  and  $(S_i, S_j) \in E_C$  if and only if there exists an edge in  $G$  from some vertex in  $S_i$  to some vertex in  $S_j$ .  $G_C$  is consequently a coarser graph with the hierarchical structure preserved [21].

## 3. Problem Statement

We consider a discrete time dynamical system described by  $\mathbf{x}[k+1] = \mathbf{S}(\mathbf{x}[k], \mathbf{u}[k])$ , where  $\mathbf{x}[k] \in \mathbb{R}^n$  is the state and  $\mathbf{u}[k] \in \mathbb{R}^l$  is the control input at time  $k$ . We collect the consecutive measurements  $\{\mathbf{x}[i]\}_{i=1}^{m+1}$  and  $\{\mathbf{u}[i]\}_{i=1}^m$  from the system and we assume a dictionary of observables  $\phi = [\phi_1 \dots \phi_L]^T$

exists. The goal is to find a subset  $\bar{\phi} \in \cup\{\phi_i\}_{i=1}^L$  such that  $\bar{\phi}$  is the smallest dictionary which includes all the observables affecting the output variables of the Koopman model.

Our goal requires inference of both the entries of  $\hat{\mathbf{K}}_F$  in (4) and another matrix of the same size indicating whether the corresponding element should be included in the regression. We therefore adopt a probabilistic spike and slab type model [22] and use VB inference to estimate the posterior distribution of model parameters. Assuming the dynamical system has control inputs, we define the design matrix as  $\Phi = [\Phi' | \mathbf{U}] \in \mathbb{R}^{m \times (L+l)}$  where  $[\Phi']_{ij} = \phi_j(\mathbf{x}[i])$  for all  $1 \leq i \leq m, 1 \leq j \leq L$  and  $[\mathbf{U}]_{ij} = u_j[i]$  for all  $1 \leq j \leq l$ . Then, we treat the Koopman model regression of each dictionary element as an independent problem by setting the target regression variable  $\mathbf{t}_j = [\phi_j(\mathbf{x}[2]) \dots \phi_j(\mathbf{x}[m+1])]^T$  for each  $1 \leq j \leq L$  so that

$$\mathbf{t}_j = \Phi(\boldsymbol{\gamma}_j \odot \boldsymbol{\beta}_j) + \mathbf{v}_j \quad \mathbf{v}_j \sim \mathcal{N}(\mathbf{0}, \rho_j^{-1} \mathbf{I}_{m \times m}), \quad (8)$$

where  $\boldsymbol{\gamma}_j$  is the vector of inclusion flags and  $\boldsymbol{\beta}_j$  is the vector of weights corresponding to each column of  $\Phi$ , respectively. We then add a new level of hierarchy to our probabilistic model by assigning conditional priors to the coefficients  $\boldsymbol{\beta}_j$  and  $\boldsymbol{\gamma}_j$ . In particular, we model  $\boldsymbol{\beta}_j$  as a vector of independent Gaussian random variables with zero mean and unknown precision as

$$\boldsymbol{\beta}_j \sim \prod_{i=1}^{L+l} \mathcal{N}(\beta_{j,i}; 0, \alpha_{j,i}^{-1}). \quad (9)$$

Then, we model the inclusion vector  $\boldsymbol{\gamma}_j$  as independent Bernoulli distributions to represent its binary nature:

$$\boldsymbol{\gamma}_j \sim \prod_{i=1}^{L+l} \text{Bernoulli}(\gamma_{j,i}; \pi_{j,i}). \quad (10)$$

Finally, we complete the hierarchy by assigning priors to the hyperparameters in our model; namely,  $\rho_j$ ,  $\alpha_{j,i}$  and  $\pi_{j,i}$  for each  $j$  and  $i$ . Gamma distribution, given by the shape and rate parameters, is the conjugate prior for the precision hyperparameter of Gaussian distribution [18], so we assign  $\rho_j$  and  $\alpha_{j,i}$  Gamma distributions:

$$\rho_j \sim \text{Gamma}(\rho_j; a_j, b_j), \quad (11)$$

$$\alpha_j \sim \prod_{i=1}^{L+l} \text{Gamma}(\alpha_{j,i}; c_{j,i}, d_{j,i}). \quad (12)$$

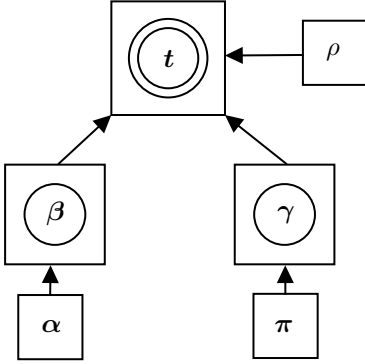


Figure 1: The hierarchy of the random variables in the proposed model.

Similarly, the conjugate prior of Bernoulli distribution is the Beta distribution [18]. Consequently, we assign the prior distribution of  $\pi_{j,i}$  as:

$$\pi_j \sim \prod_{i=1}^{L+l} \text{Beta}(\pi_{j,i}; e_{j,i}, f_{j,i}), \quad (13)$$

We estimate the posterior of all random variables by VB inference separately for each  $1 \leq j \leq L$ . The complete hierarchy for a given target variable is depicted in Figure 1. Once the estimation of random variables is complete, we use the estimates of the random variables to construct  $\hat{\mathbf{K}}_F = [\hat{\gamma}_1 \odot \hat{\beta}_1 \mid \dots \mid \hat{\gamma}_L \odot \hat{\beta}_L]$  and obtain the probabilistic Koopman model:

$$\phi(\mathbf{x}[k+1])^T = [\phi(\mathbf{x}[k])^T \mathbf{u}[k]^T] \hat{\mathbf{K}}_F + \mathbf{v}^T \quad (14)$$

where  $\mathbf{v} \sim \mathcal{N}(\mathbf{0}, \text{diag}(\hat{\rho}_1^{-1}, \dots, \hat{\rho}_L^{-1}))$ . As the last step of our task, we utilize the so called inclusion matrix  $\mathbf{\Gamma} = [\hat{\gamma}_1 \mid \dots \mid \hat{\gamma}_L]$  to find  $\bar{\phi}$ .

## 4. Method

### 4.1. VB inference of posterior distributions

The equations (8)–(13) set up the prior model. We seek the estimates of the posterior distributions of each random variable in each of the  $L$ -many independent problems. Since the problems are identical for each of the  $L$ -many targets variables  $\{\mathbf{t}_j\}_{j=1}^L$ , we drop the subscript  $j$  in all the random variables for brevity. The posterior estimation approach allows our model to take shape according to the data. In particular, we set the prior of  $\beta_i$  to a zero mean Gaussian with random variable precision, which reflects the prior indifference about the coefficients of

the model. This approach also promotes sparsity, acting as a regularizer because the posterior stays zero mean unless there is data to prove otherwise.

The exact posterior distribution of all parameters is costly to find. We therefore treat the random variables in our model as hidden variables and resort to the mean field approximation (6). Accordingly,

$$p(\beta, \gamma, \alpha, \pi, \rho \mid \mathbf{t}) \approx q(\rho) \prod_{i=1}^{L+l} q(\beta_i) q(\gamma_i) q(\alpha_i) q(\pi_i), \quad (15)$$

where each  $q(\cdot)$  inherits the corresponding distribution type of the same random variable in our model prior. This means for each  $1 \leq i \leq (L+l)$ ,  $q(\beta_i)$ ,  $q(\gamma_i)$ ,  $q(\alpha_i)$  and  $q(\pi_i)$  are Gaussian, Bernoulli, Gamma and Beta distributions, respectively. Likewise,  $q(\rho)$  is a Gamma distribution. Consequently, (7) applies for posterior estimation. Our model prior allows the conditional decomposition of the joint distribution as

$$\begin{aligned} p(\mathbf{t}, \beta, \gamma, \alpha, \pi, \rho) = \\ p(\mathbf{t} \mid \beta, \gamma, \rho) p(\beta \mid \alpha) p(\gamma \mid \pi) p(\alpha) p(\pi) p(\rho). \end{aligned} \quad (16)$$

The VB inference procedure starts from an initial set  $\{a, b, \{c_i, d_i, e_i, f_i, \alpha_i, \mu_i, \pi_i\}_{i=0}^{L+l}\}$  for the model parameters. Then, we perform updates iteratively in the Jacobi fashion to allow for parallelization [23].

We denote by the barred variables the posterior parameter estimates after the update takes place and by hat variables the expectations of the random variables after the previous iteration. The symbol  $\pm$  is used to indicate that the equation holds up to an additive constant.

#### 4.1.1. Update of $q(\rho)$

Starting with the update regarding  $q(\rho)$ , we derive

$$\log q(\rho) \stackrel{\pm}{=} \mathbb{E}_{q \setminus \rho} [\log p(\mathbf{t} \mid \beta, \gamma, \rho) + \log p(\rho)] \quad (17a)$$

$$\stackrel{\pm}{=} \mathbb{E}_{q \setminus \rho} \left[ \frac{m}{2} \log \rho - \frac{\rho}{2} \|\mathbf{t} - \Phi(\gamma \odot \beta)\|^2 + (a-1) \log \rho - b\rho \right], \quad (17b)$$

$$\implies q(\rho) \propto \rho^{\bar{a}-1} e^{-\bar{b}\rho}, \text{ where} \quad (17c)$$

$$\bar{a} = \frac{m}{2} + a \text{ and } \bar{b} = \frac{1}{2} \|\mathbf{t} - \Phi(\hat{\gamma} \odot \mu)\|^2 + b. \quad (17d)$$

#### 4.1.2. Update of $q(\alpha_i)$

We continue with the update for  $q(\alpha_i)$ .

$$\log q(\alpha_i) \stackrel{+}{=} \mathbb{E}_{q_{\setminus \alpha_i}} [\log p(\beta | \alpha) + \log p(\alpha)] \quad (18a)$$

$$\stackrel{+}{=} \mathbb{E}_{q_{\setminus \alpha_i}} \left[ \frac{1}{2} \log \alpha_i - \frac{\alpha_i}{2} \beta_i^2 + (c_i - 1) \log \alpha_i - d_i \alpha_i \right] \quad (18b)$$

$$\implies q(\alpha_i) \propto \alpha_i^{\bar{c}_i - 1} e^{-\bar{d}_i \alpha_i} \text{ where} \quad (18c)$$

$$\bar{c} = c_i + \frac{1}{2} \text{ and } \bar{d}_i = d_i + \frac{\mu_i^2 + \sigma_i^2}{2}. \quad (18d)$$

#### 4.1.3. Update of $q(\pi_i)$

Next, we investigate the update of  $q(\pi_i)$ .

$$\log q(\pi_i) \stackrel{+}{=} \mathbb{E}_{q_{\setminus \pi_i}} [\log p(\gamma | \pi) + \log p(\pi)] \quad (19a)$$

$$\stackrel{+}{=} \mathbb{E}_{q_{\setminus \pi_i}} [(\gamma_i + e_i - 1) \log \pi_i + (1 - \gamma_i + f_i - 1) \log (1 - \pi_i)] \quad (19b)$$

$$\implies q(\pi_i) \propto \pi_i^{(\bar{e}_i - 1)} (1 - \pi_i)^{\bar{f}_i - 1}, \text{ where} \quad (19c)$$

$$\bar{e}_i = \hat{\gamma}_i + e_i \text{ and } \bar{f}_i = 1 - \hat{\gamma}_i + f_i. \quad (19d)$$

#### 4.1.4. Update of $q(\beta_i)$

Then, we move on to the update of  $q(\beta_i)$ . In this regard, we assume that  $q(\beta_i)$  is Gaussian distributed with mean  $\mu_i$  and covariance  $\alpha_i^{-1}$ . Now, we evaluate the expectation (7):

$$\log q(\beta_i) \stackrel{+}{=} \mathbb{E}_{q_{\setminus \beta_i}} [\log p(t | \beta, \gamma, \rho) + \log p(\beta | \alpha)] \quad (20a)$$

$$\begin{aligned} &\stackrel{+}{=} \mathbb{E}_{q_{\setminus \beta_i}} \left[ \sum_{k=1}^m \frac{-\rho}{2} \left( \gamma_i \beta_i \phi_i^2(\mathbf{x}[k]) \right. \right. \\ &\quad \left. \left. - 2\gamma_i \beta_i \phi_i(\mathbf{x}[k]) \left( t_k - \sum_{\substack{j=1 \\ j \neq i}}^{L+l} \gamma_j \beta_j \phi_j(\mathbf{x}[k]) \right) \right) - \frac{\alpha_i}{2} \beta_i^2 \right]. \end{aligned} \quad (20b)$$

For notational simplicity, we define the residual of the  $k$ -th target variable without the  $i$ -th coefficient:

$$r_{ik} = \left( t_k - \sum_{\substack{j=1 \\ j \neq i}}^{L+l} \gamma_j \beta_j \phi_j(\mathbf{x}[k]) \right). \quad (21)$$

Then by arranging the terms in a tidy manner, we obtain

$$\begin{aligned} \log q(\beta_i) &\stackrel{+}{=} \mathbb{E}_{q_{\setminus \beta_i}} \left[ \beta_i^2 \left( \sum_{k=1}^m \frac{-\rho}{2} \gamma_i \phi_i^2(\mathbf{x}[k]) - \frac{\alpha_i}{2} \right) + \right. \\ &\quad \left. \beta_i \left( \sum_{k=1}^m \rho \gamma_i \phi_i(\mathbf{x}[k]) r_{ik} \right) \right]. \end{aligned} \quad (22)$$

Taking the expectation with respect to all random variables except  $\beta_i$ , we obtain the posterior estimates

$$\bar{\alpha}_i = \sum_{k=1}^m \hat{\rho} \hat{\gamma}_i \phi_i^2(\mathbf{x}[k]) + \hat{\alpha}_i, \quad (23a)$$

$$\bar{\mu}_i = \frac{\sum_{k=1}^m \hat{\rho} \hat{\gamma}_i \phi_i(\mathbf{x}[k]) \hat{r}_{ik}}{\sum_{k=1}^m \hat{\rho} \hat{\gamma}_i \phi_i^2(\mathbf{x}[k]) + \hat{\alpha}_i}. \quad (23b)$$

In our implementations, we have seen the benefit of introducing damping to the updates for  $\mu_i$  and  $\alpha_i$ . This technique is used in the literature where the loss surface is rugged [24]. With the introduction of damping coefficient  $p_d \in (0, 1)$ , updates become:

$$\bar{\alpha}_{i-\text{damped}} = p_d \bar{\alpha}_i + (1 - p_d) \bar{\alpha}_{i-1}, \quad (24a)$$

$$\bar{\mu}_{i-\text{damped}} = p_d \bar{\mu}_i + (1 - p_d) \bar{\mu}_{i-1}. \quad (24b)$$

#### 4.1.5. Update of $q(\gamma_i)$

As the last step, we derive the posterior hyper-parameter estimates regarding  $q(\gamma_i)$ .

$$\log q(\gamma_i) \stackrel{+}{=} \mathbb{E}_{q_{\setminus \gamma_i}} [\log p(t | \beta, \gamma, \rho) + \log p(\gamma | \pi)] \quad (25a)$$

$$\begin{aligned} &\stackrel{+}{=} \mathbb{E}_{q_{\setminus \gamma_i}} \left[ \frac{-\rho}{2} \sum_{k=1}^m (r_{ik} - \gamma_i \beta_i \phi_i(\mathbf{x}[k]))^2 \right. \\ &\quad \left. + \gamma_i \log(\pi_i) + (1 - \gamma_i) \log(1 - \pi_i) \right], \end{aligned} \quad (25b)$$

where  $r_{ik}$  is defined as in (21). We can stack  $r_{ik}$  in a vector

$$\mathbf{r}_i = [r_{i1} \quad \dots \quad r_{im}]^T \text{ for } i = 1, \dots, L. \quad (26)$$

We then write  $\log q(\gamma_i)$  more compactly:

$$\begin{aligned} \log q(\gamma_i) &\stackrel{+}{=} \mathbb{E}_{q_{\setminus \gamma_i}} \left[ \frac{-\rho}{2} (-2\gamma_i \beta_i \phi_i^T \mathbf{r}_i + \gamma_i \beta_i^2 \|\phi_i\|^2) \right. \\ &\quad \left. + \gamma_i \log(\pi_i) + (1 - \gamma_i) \log(1 - \pi_i) \right]. \end{aligned} \quad (27)$$

Taking the expectation,

$$\begin{aligned} \log q(\gamma_i) &\stackrel{+}{=} \frac{-\hat{\rho}}{2} (-2\gamma_i \mu_i \phi_i^T \hat{\mathbf{r}}_i + \gamma_i (\mu_i^2 + \sigma_i^2) \|\phi_i\|^2) \\ &\quad + \gamma_i (\psi(\hat{e}_i) - \psi(\hat{f}_i)), \end{aligned} \quad (28)$$

where

$$\begin{aligned}\mathbb{E}_{\pi_i}[\log(\pi_i)] &= \psi(\hat{e}_i) - \psi(\hat{e}_i + \hat{f}_i), \\ \mathbb{E}_{\pi_i}[\log(1 - \pi_i)] &= \psi(\hat{f}_i) - \psi(\hat{e}_i + \hat{f}_i),\end{aligned}\quad (29)$$

and  $\psi(\cdot)$  is the Digamma function [25]. Since the expectation is taken with respect to the posterior density of  $\pi_i$ , the hyperparameters  $\hat{e}_i$  and  $\hat{f}_i$  in (29) should be the posterior estimates. Continuing from (28), we group the terms together and simply avoid the constant terms since they can be normalized:

$$\log q(\gamma_i) = \gamma_i \eta_i, \quad (30)$$

where

$$\eta_i = \hat{\rho} \mu_i \phi_i^T \hat{r}_i - \frac{1}{2} \hat{\rho} (\mu_i^2 + \sigma_i^2) \|\phi_i\|^2 + \psi(\hat{e}_i) - \psi(\hat{f}_i). \quad (31)$$

Since we model the posterior distribution of  $\gamma_i$  as a Bernoulli distribution,  $\gamma_i$  can take values in  $\{0, 1\}$ . Then we may write

$$\begin{aligned}q(\gamma_i) &\propto e^{\gamma_i \eta_i}, \\ \bar{\pi}_i &= q(\gamma_i = 1) \propto e^{\eta_i}, \\ 1 - \bar{\pi}_i &= q(\gamma_i = 0) \propto 1.\end{aligned}\quad (32)$$

By normalizing, we derive the posterior estimate of  $\bar{\pi}_i$ :

$$\bar{\pi}_i = \frac{e^{\eta_i}}{1 + e^{\eta_i}} = \frac{1}{1 + e^{-\eta_i}} = \sigma(\eta_i), \quad (33)$$

where  $\sigma(\cdot)$  is the sigmoid function [18]. Here, we have experimentally observed the improved numerical stability when we clip  $\pi_i$  between  $[\delta, 1 - \delta]$  where  $\delta$  is a small number, such as  $10^{-8}$ .

#### 4.2. Dictionary Reduction Using The Inclusion Matrix

The  $\gamma$  random variable in (8) serves to represent the model's belief about whether the corresponding observable value is significant for the target variable. In a sense, it describes existence. Once the regression problem (8) is solved for all  $L$ -many independent target variables and all random variable estimates, we actually obtain a matrix of existence made up of  $\gamma_i$  vectors such that we denote this matrix of existence as  $\Gamma = [\hat{\gamma}_1 \mid \dots \mid \hat{\gamma}_L]$ .  $\Gamma$  is essentially made up of near 0 and near 1 entries after the iterations converge since the sparsity promoting prior for  $\pi$  pulls the posterior beliefs towards either value whenever there is enough evidence to suggest so.

---

#### Algorithm 1 VB Inference for the Proposed Model for a Given Target Type $k$

---

**Require:**  $\Phi, t, a, b, \{c_i\}_{i=1}^{L+l}, \{d_i\}_{i=1}^{L+l}, \{e_i\}_{i=1}^{L+l}, \{f_i\}_{i=1}^{L+l}, p_d$

- 1: Initialize  $q(\beta_i), q(\gamma_i), q(\alpha_i), q(\pi_i), q(\rho)$  for all  $i$ .
- 2: **repeat**
- 3:     Update  $q(\rho)$  using (17d)
- 4:     **for**  $i = 1$  to  $L + l$  **do**
- 5:         Update  $q(\alpha_i)$  using (18d)
- 6:         Update  $q(\pi_i)$  using (19d)
- 7:         Compute the residual using (21)
- 8:         Update  $q(\beta_i)$  using (23)
- 9:         Damping update for  $q(\beta_i)$  using (24)
- 10:         Update  $q(\gamma_i)$  using (31), (33)
- 11:         Update the expectations:
- 12:          $\hat{\rho} = \frac{\bar{a}}{b}$
- 13:          $\hat{\alpha}_i = \frac{\bar{c}}{d}$
- 14:          $\hat{\pi}_i = \frac{\bar{e}}{\bar{e} + \bar{f}}$
- 15:          $\sigma_i^2 = \bar{\alpha}_i^{-1}$
- 16:          $\beta_i \sim \mathcal{N}(\bar{\mu}_{i-\text{damped}}, \sigma_i^2)$
- 17:          $\hat{\gamma}_i = \bar{\pi}_i$
- 18:     **end for**
- 19:     **until** Maximum number of iterations is reached or  $q(\beta_i)$  converged
- 20: **return** Posteriors  $q(\beta), q(\gamma), q(\alpha), q(\pi), q(\rho)$

---

The entries of  $\Gamma$  can be viewed as probabilities that a given state affects others. Assuming we want to prune the dictionary in a way that eliminates the entries of  $\hat{\mathbf{K}}_F$  that have less than  $\epsilon$  probability of being included in the regression, we may easily threshold these probabilities since they are scale free. We can therefore flag the discarded entries 0 while others get assigned 1. Denote this threshold matrix as  $\Gamma^\epsilon$ :

$$[\Gamma^\epsilon]_{ij} = \begin{cases} 0 & \text{if } [\Gamma]_{ij} < \epsilon \\ 1 & \text{if } [\Gamma]_{ij} \geq \epsilon \end{cases}. \quad (34)$$

Clearly,  $\Gamma^\epsilon$  contains only 0s and 1s, yielding a proper adjacency matrix of a directed graph where the nodes are the states of the dynamical Koopman model. So, if an edge from state  $i$  to state  $j$  exists,  $\phi_i$  is present in the regression for  $\phi_j$ . In that case,  $\Gamma_{ij}^\epsilon = 1$ . On the other hand, if  $\phi_i$  is absent in the regression for  $\phi_j$ , then  $\Gamma_{ij}^\epsilon = 0$  and the edge between them does not exist.

Switching to the graph perspective allows for the use of existing graph notions such as connectivity. With a slight abuse of notation we say a node  $m$  is the ancestor of a node  $k$  if  $k$  is reachable from

$m$ . We denote the ancestors of node  $k$  as  $\mathcal{A}(k)$ . It may happen that a node is included in a SCC but some ancestors of the node are outside the component. We may therefore consider that each SCC also has a reachability property just like nodes. In the dynamical model sense, all states have impact on all others inside a SCC but they may be affected by some states in other components. Adopting the condensed graph perspective reduces the number of nodes and groups subsystems together [17]. Therefore, it is better to approach the problem from the SCC perspective. Let  $\{S_i\}_{i=1}^N$  be the SCCs of a graph. There exists a condensed graph where nodes are  $\{S_i\}_{i=1}^N$  and edges exist whenever a SCC is reachable from another. Condensed graph essentially sets all nodes inside a SCC as equivalent and roughens the topology.

The procedure to reduce the Koopman model dimension is then straightforward. We propose Algorithm 2. The algorithm starts with an initial full sized Koopman model of the form (4), where the states that are included in the output of the model are indexed with a finite index set  $\mathcal{O}$ . The model is identified through the proposed spike and slab approach via VB inference so that the inclusion matrix  $\Gamma$  is explicitly given to the algorithm. We then require a probability threshold below which the algorithm discards the corresponding entry of the matrix  $\hat{\mathbf{K}}_F$ . The proposed algorithm starts by obtaining the adjacency matrix  $\Gamma^\epsilon$ . Then, the condensed graph, namely the graph of the SCCs is built. The reduced dictionary is constructed by including the SCCs that contain the output states  $\{\phi_\lambda\}_{\lambda \in \mathcal{O}}$  and all of the ancestors of these SCCs. The ancestry search can be handled via any preferred graph search algorithm.

## 5. Results

We compare the results of various Koopman EDMD identification methods with full sized and reduced dictionaries across a representative spectrum of systems to demonstrate the performance gain of our method on existing approaches when used as an aiding module. To keep the discussion structured, we elaborate on each system and the respective implementation details in the related subsections. For all methods, we demonstrate the results of ordinary least squares solutions as given in [5], sequential thresholded least squares [14] solutions, Sparse Bayesian Learning (SBL) solutions

---

### Algorithm 2 Dictionary Reduction via Graph Structure

---

**Require:** Koopman model (4) with outputs  $\{\phi_\lambda\}_{\lambda \in \mathcal{O}}$ ; posterior estimate of inclusion matrix  $\Gamma$ ; threshold  $\epsilon > 0$ . Reduced dictionary  $\bar{\phi}$ .

- 1: Identify the nodes corresponding to the outputs  $\{\phi_\lambda\}_{\lambda \in \mathcal{O}}$  of the Koopman model (4), where  $\mathcal{O}$  is the finite index set of output nodes.
- 2: Threshold the posterior estimate of the existence matrix  $\Gamma$  by  $\epsilon$  to obtain  $\Gamma^\epsilon$ .
- 3: Compute the strongly connected components (SCCs)  $\{S_i\}_{i=1}^M$  of the graph  $\mathcal{G}$  represented by  $\Gamma^\epsilon$ .
- 4: Construct the condensed graph  $\mathcal{G}_c$  whose nodes are the SCCs  $\{S_i\}_{i=1}^M$ .
- 5: Determine the subset of SCCs  $\{S_j\}_{j=1}^{M_0}$  that contain the output nodes  $\{\phi_\lambda\}_{\lambda \in \mathcal{O}}$ .
- 6: Compute the set of ancestors  $\mathcal{A}(\{S_j\}_{j=1}^{M_0})$  in the condensed graph  $\mathcal{G}_c$ .
- 7: Construct the reduced dictionary

$$\bar{\phi} = \left\{ \phi_k \mid k \in \mathcal{O} \text{ or } \phi_k \in \mathcal{A}(\{S_j\}_{j=1}^{M_0}) \right\}.$$


---

[26] and finally the performance of the model identified with the proposed model. Although we propose our algorithm as a model selection framework, it also provides a Koopman model similarly to the other methods. Therefore, we also provide the results of the proposed Koopman model with the full and reduced dictionaries as well. In our presentations, we use the labels I, II, III, IV for the pseudoinverse as proposed in [5], sequential thresholded least squares [14], SBL [26] and the proposed method, respectively. For method II, we set the threshold parameter  $\lambda = 0.05$  for the first system,  $\lambda = 0.005$  for the second system and  $\lambda = 0.015$  for the last system. The first two systems investigated here are subject to artificially added measurement noise, the specifications of which are given in the respective sections. The same level of noise is added to all the measured states independently. This artificial measurement noise helps to examine our method's robustness against data corruption by evaluating the performance in changing signal to noise ratio (SNR) levels. For these two systems, we consider 25 Monte Carlo (MC) runs for each noise level and display the mean of the MC runs with solid lines. The shaded areas represent to the 95% confidence interval for the corresponding color. The

last experiment includes real data, already corrupt with measurement noise and process noise. Therefore, we do not add artificial noise and neither do we undertake a statistical study. Our performance metric is the one step prediction normalized mean squared error (NMSE) given by:

$$\text{NMSE}_x = \frac{\|x_{\text{true}} - x_{\text{predicted}}\|^2}{\|x_{\text{true}} - \text{mean}(x_{\text{true}})\|^2}. \quad (35)$$

For all systems, we use the measured states and squared exponential kernels in the dictionary as per [9]. The centers of the kernel sections are set as the cluster centers of the training data for a given cluster count. For the last system, we also add squared exponentials with periodic exponents to the dictionary. For the exponent coefficients and frequencies, we set values of different orders of magnitude to capture both slow and fast tendencies. Here, our discussion is on the evaluation of the dictionary and if possible reductions exist.

### 5.1. Lorenz Attractor

We begin by studying the proposed method on the Lorenz attractor. The attractor is a famous chaotic system that is commonly used as a nonlinear system identification benchmark [27]. We use simulation data of the system sampled at 1 KHz for 6 seconds for training and use unseen data for testing. For this system, the full size dictionary includes 23 observables. For brevity, we only present the results of the  $y$  state of the system as described in [14].

The average model size with respect to varying measurement noise strengths is given in Figure 2. According to this result, either the dataset is not rich enough to require 23 observables, or the selected observables do not suit the data.

Figure 3 demonstrates the NMSE performance of various methods using the full size dictionary. Next, we determine the reduced dictionary  $\bar{\phi}$  separately for each SNR level, then identify the reduced model parameters using all methods. As a result of dictionary reduction, the reduced model size is different for each noise level. In Figure 4, we present the NMSE performance of all methods after the dictionary reduction has been applied as proposed with  $\epsilon = 0.01$ . Comparing Figure 3 and Figure 4, we observe that the previously unstable performances of the methods labeled I, II have significantly improved with the reduced dictionary. On the other hand, the methods III and IV, which yielded lower

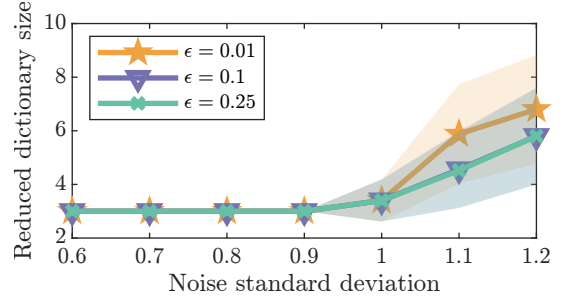


Figure 2: Reduced dictionary sizes of the Lorenz system with different  $\epsilon$  across all measurement noise levels.

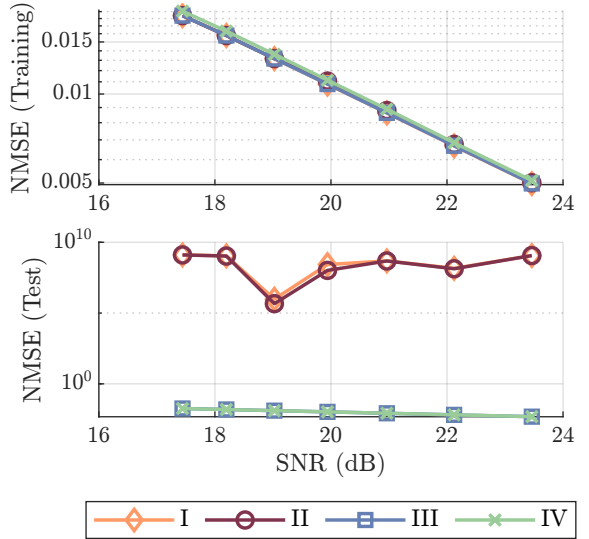


Figure 3: NMSE performance of full size models identified with different methods for the  $y$  state of the Lorenz attractor in both training and test datasets.

NMSE scores with the full size dictionary, maintain their performance even though the model dimension is reduced.

### 5.2. Underactuated Unmanned Surface Vehicle (USV)

We continue by implementing our method on an USV to demonstrate the performance on controlled systems. We use the differential drive USV as characterized in [28] in a simulation environment. We generate the data at 10 Hz sampling frequency for 200 seconds for training. In this study, only the velocity states and the control inputs are measured and included in the Koopman model. However, we add 1 time step delayed states to the measured states and apply the observables to this combined state. The full size dictionary includes 28 observ-

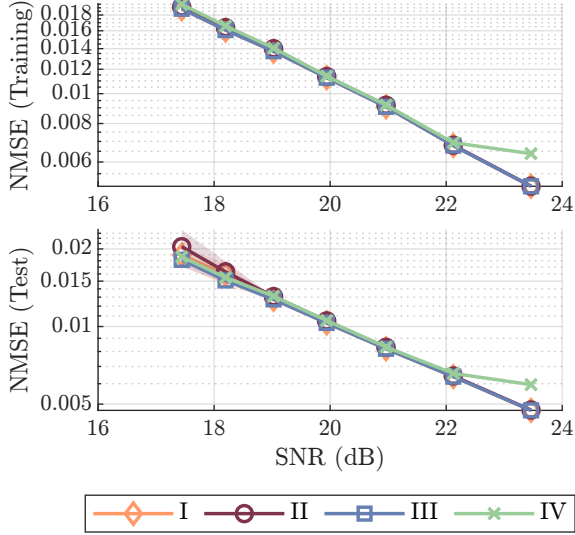


Figure 4: NMSE performance of reduced size models identified with different methods for the  $y$  state of the Lorenz attractor in both training and test datasets.

ables of state and 2 control inputs. Dictionary reduction is not performed on the control inputs in any case. To keep the exposition focused, we report results for only the surge velocity state; the remaining velocity components exhibit the same trend.

We provide the NMSE performance of all considered techniques using the full size dictionary in Figure 5. This figure demonstrates that performances of all methods are comparable in lower SNR values while VB inference method saturates learning in high SNR intervals. The proposed hierarchical model also exhibits larger variance as indicated by the shaded area. It could be since the model is more expressive when compared to the other techniques. We now provide NMSE performances of the methods with reduced dictionaries by setting  $\epsilon = 0.25$  in Figure 6. This is a more strict threshold when compared to the threshold we imposed for the Lorenz system. Comparing the full size model results in Figure 5 with the reduced size model results in Figure 6, only minor differences are seen. The variance of the VB based method has reduced in the reduced model case, indicating that the full size model was too expressive for high SNR data to be handled in the spike and slab sense. The performance of all the methods are largely unaltered by the reduced dictionary size. The contribution of our method is therefore clear here, same performance is achieved through a smaller state space. In particular, we present the dictionary sizes for three differ-

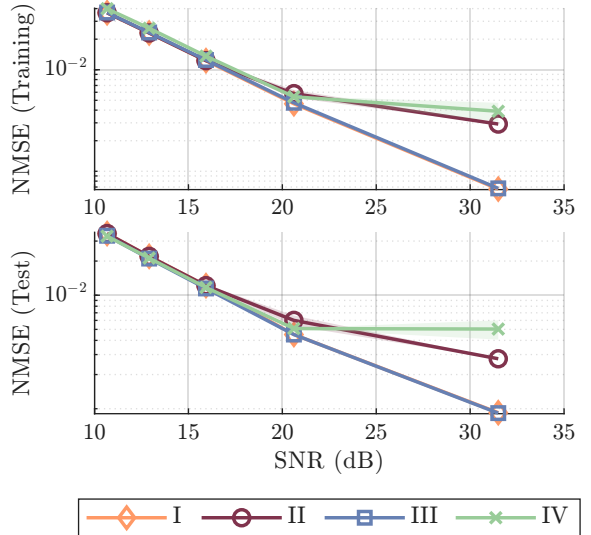


Figure 5: NMSE performance of full size models identified with different methods for the surge velocity state of USV in both training and test datasets.

ent  $\epsilon$  thresholds for varying artificial measurement noise levels in Figure 7. As observed in Figure 7, the same performance can be achieved with as few as 10 observables using the same data. Moreover, the threshold level is observed to have negligible impact on the results, indicating that  $\hat{\gamma}$  values converged to near 0 values whenever necessary. In other words, they are not indeterminate.

### 5.3. Wiener-Hammerstein Process Noise System

Our final case study is the real data collected from a Wiener-Hammerstein system. The system is a nonlinear operational amplifier-resistor network wrapped in between two LTI filters. The filter at the output features a zero that is included in the input excitation frequency range. The system is also subjected to both process and measurement noise injected via external sources, with process noise being the dominant disturbance. The static nonlinearity caused by the diode networks is notoriously difficult to diagnose because the saturation causes information loss. Input signals with varying amplitudes and frequencies are used to capture the hybrid dynamics. Another challenge in identifying this system is that the process noise enters before the nonlinear network, strengthening unpredictability [29].

The full size dictionary consists of 46 observables and one dimensional control input. We apply our proposed dictionary reduction method by setting

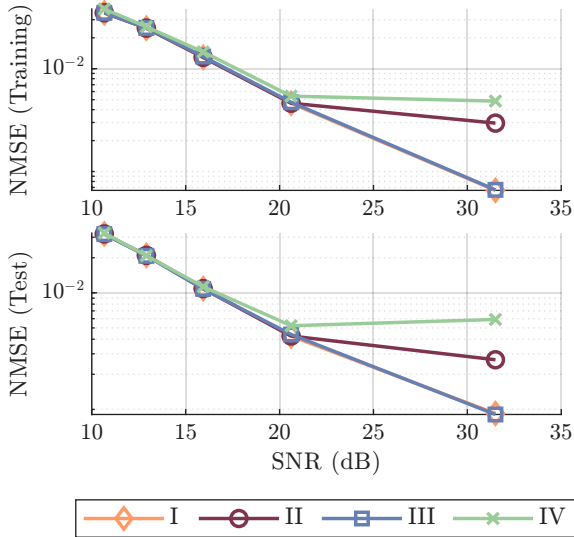


Figure 6: NMSE performance of reduced size models identified with different methods for the surge velocity state of USV in both training and test datasets.

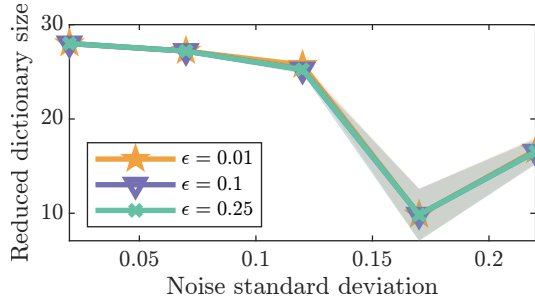


Figure 7: Reduced dictionary sizes of the USV with different  $\epsilon$  across all measurement noise levels.

$\epsilon = 0.1$  and consequently reduce the dictionary to 8 observables. The one step prediction NMSE of three of the methods are identical with the full size dictionary and with the reduced dictionary. Proposed Koopman model identification method has higher one step prediction errors in the reduced model compared to the full size model. For comparison, we provide NMSE scores in Table 1. Other methods have outperformed the proposed inference method in both the full size and the reduced size models. However, for many systems applications, one step prediction performance can possibly be misleading [8]. We therefore examine the identified  $\hat{\mathbf{K}}_F$  matrices for each method. Note that the columns of  $\hat{\mathbf{K}}_F$  correspond to the elementwise product of  $\boldsymbol{\mu}_i = \hat{\boldsymbol{\beta}}_i$  and  $\hat{\boldsymbol{\gamma}}_i$  where  $i$  is the column index. In Figure 8, we present the heatmap of the the

	Training	Test
<b>Full</b>		
<b>I</b>	$9.9 \times 10^{-3}$	$4.5 \times 10^{-3}$
<b>II</b>	$10^{-4}$	$4.6 \times 10^{-3}$
<b>III</b>	$9.9 \times 10^{-3}$	$4.5 \times 10^{-3}$
<b>IV</b>	$10^{-4}$	$4.6 \times 10^{-3}$
<b>Reduced</b>		
<b>I</b>	$9.9 \times 10^{-3}$	$4.5 \times 10^{-3}$
<b>II</b>	$10^{-4}$	$4.6 \times 10^{-3}$
<b>III</b>	$9.9 \times 10^{-3}$	$4.5 \times 10^{-3}$
<b>IV</b>	$1.27 \times 10^{-4}$	$7.3 \times 10^{-3}$

Table 1: One step prediction NMSE scores of Koopman models for the Wiener-Hammerstein process noise system identified with 4 different methods using the full and the reduced dictionaries.

absolute values of the entries of  $\hat{\mathbf{K}}_F$  found with different methods using the full sized dictionary. It is clear that despite the seemingly successful one step NMSE performances, methods I and II suffer severely from numerical instabilities. On the other hand, method III achieves to recover a smoother matrix. Method IV, which is the proposed matrix inference method, has entries with very low orders of magnitude. This is because we clip the values of  $\gamma$  at  $10^{-8}$  in our implementation. Nonetheless, it is clear that method IV manages to sparsify the dynamics without suffering from overfitting. It can also be argued that the model priors are set such that method IV prefers sparsity more strongly than method III. Next, we prune the dictionary using the proposed dictionary reduction algorithm. Then, we present the heatmap of the recovered matrices with the reduced dictionary using each method in Figure 9. Compared to Figure 8, the ill conditioning of the methods I and II has significantly resolved.

## 6. Conclusion

In this work, we have proposed a hierarchical probabilistic model for Koopman model identification of discrete time dynamical systems. We treat the regression of the time evolution of each observable independently from others. The main distinction of our model is the incorporation of inclusion random variables, which take binary values. This random variable multiplies the regression coefficients, effectively discarding or keeping each observable. The hyperparameter estimates of the

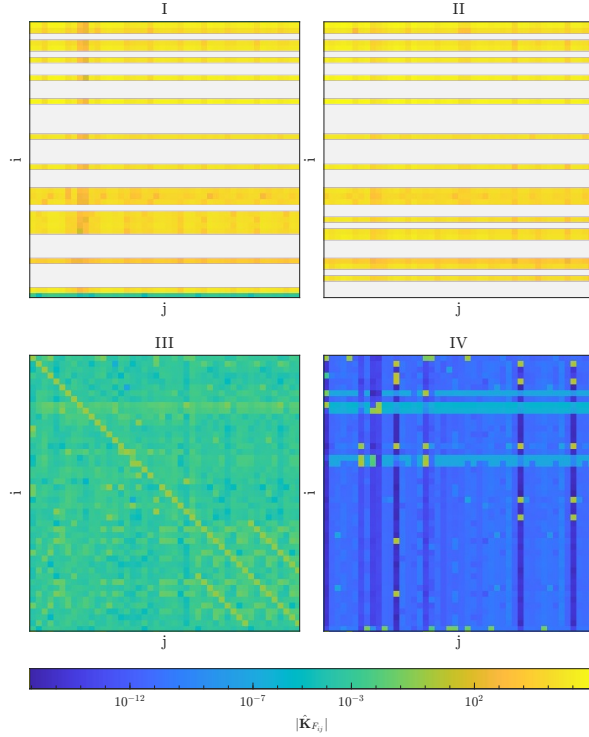


Figure 8: Heatmap of the recovered  $|\hat{\mathbf{K}}_F|$  matrices of different methods using the full sized dictionary. Gray indicates zero entries.

weights, inclusion flags and resulting regression error are also treated randomly and inferred. For inference of the random variables, we use VB updates. Finally, when the inclusion variables for all observables and in each observable regression problems are estimated, we get a matrix of flag probabilities. We apply thresholds on the probabilities to get a binary matrix. This binary matrix is interpreted as the adjacency matrix of a directed graph, where each vertex is an observable of the Koopman model. By finding all the ancestors of the outputs of the Koopman model in the condensed graph, we obtain the subset of the initial dictionary that is relevant for output prediction. The performance of our method is evaluated in three representative systems. In the Lorenz attractor simulation we demonstrate that the reduced dictionary helps against overfitting. In the controlled USV case, we demonstrate that smaller dictionaries maintain the prediction performance. Lastly in the real experimental data of the Wiener Hammerstein process, we demonstrate that the reduced dictionary considerably improves numerical condi-

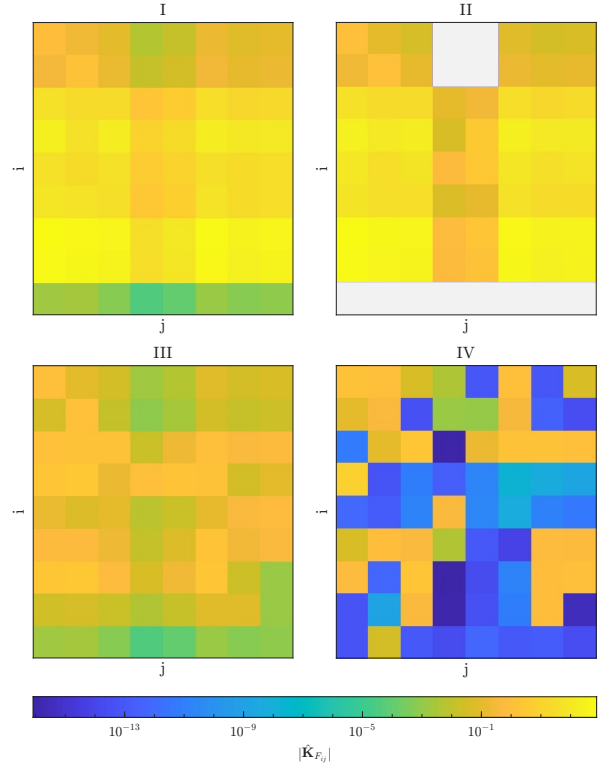


Figure 9: Heatmap of the recovered  $|\hat{\mathbf{K}}_F|$  matrices of different methods using the reduced sized dictionary. Gray indicates zero entries.

tioning. On the other hand, our method requires prior tuning for many variables. We recommend using uninformative priors and fine tuning for specific needs. Prior tuning can help in setting the belief certain observables if they are guaranteed to be included in the model. Moreover, our posterior estimates are approximated with the mean field assumption, which can be limiting. We also propose a ready to use Koopman model apart from the dictionary reduction algorithm. This model is seen to perform slightly worse than [26], especially in high SNR settings. We therefore recommend first reducing an initially large dictionary using our reduction method, then following with a robust, less complex hierarchical model such as in [26].

## 7. Acknowledgments

This work is partially funded by The Scientific and Technological Research Council of Türkiye (TÜBİTAK) with the project number 124E232 and

partially funded by Health Institutes of Türkiye (TÜSEB) with the project number 40908.

## References

- [1] L. Shi, M. Haseli, G. Mamakoukas, D. Bruder, I. Abraham, T. Murphey, J. Cortes, K. Karydis, Koopman operators in robot learning, arXiv preprint arXiv:2408.04200 (2024).
- [2] B. O. Koopman, Hamiltonian systems and transformation in hilbert space, Proceedings of the National Academy of Sciences 17 (5) (1931) 315–318.
- [3] A. Mauroy, Y. Susuki, I. Mezic, Koopman operator in systems and control, Vol. 484, Springer, 2020.
- [4] P. J. Schmid, Dynamic mode decomposition of numerical and experimental data, Journal of fluid mechanics 656 (2010) 5–28.
- [5] M. O. Williams, I. G. Kevrekidis, C. W. Rowley, A data–driven approximation of the koopman operator: Extending dynamic mode decomposition, Journal of Nonlinear Science 25 (6) (2015) 1307–1346.
- [6] J. L. Proctor, S. L. Brunton, J. N. Kutz, Generalizing Koopman theory to allow for inputs and control, SIAM Journal on Applied Dynamical Systems 17 (1) (2018) 909–930.
- [7] I. Abraham, G. De La Torre, T. D. Murphey, Model-based control using Koopman operators, arXiv preprint arXiv:1709.01568 (2017).
- [8] J. Pan, D. Li, J. Wang, P. Zhang, J. Shao, J. Yu, Autogeneration of mission-oriented robot controllers using bayesian-based koopman operator, IEEE Transactions on Robotics 40 (2024) 903–918. doi:10.1109/TRA.2023.3344033.
- [9] M. Khosravi, Representer theorem for learning Koopman operators, IEEE Transactions on Automatic Control 68 (5) (2023) 2995–3010. doi:10.1109/TAC.2023.3242325.
- [10] B. Lusch, J. N. Kutz, S. L. Brunton, Deep learning for universal linear embeddings of nonlinear dynamics, Nature Communications 9 (1) (2018) 4950.
- [11] Q. Li, F. Dietrich, E. M. Boltt, I. G. Kevrekidis, Extended dynamic mode decomposition with dictionary learning: A data-driven adaptive spectral decomposition of the Koopman operator, Chaos: An Interdisciplinary Journal of Nonlinear Science 27 (10) (2017).
- [12] N. C. Thompson, K. Greenewald, K. Lee, G. F. Manso, The computational limits of deep learning (2022). arXiv:2007.05558. URL <https://arxiv.org/abs/2007.05558>
- [13] D. G. Tzikas, A. C. Likas, N. P. Galatsanos, The variational approximation for Bayesian inference, IEEE Signal Processing Magazine 25 (6) (2008) 131–146. doi:10.1109/MSP.2008.929620.
- [14] S. L. Brunton, J. L. Proctor, J. N. Kutz, Discovering governing equations from data by sparse identification of nonlinear dynamical systems, Proceedings of the national academy of sciences 113 (15) (2016) 3932–3937.
- [15] S. Watanabe, Tree-structured parzen estimator: Understanding its algorithm components and their roles for better empirical performance (2025). arXiv:2304.11127. URL <https://arxiv.org/abs/2304.11127>
- [16] R. Nayek, R. Fuentes, K. Worden, E. Cross, On spike-and-slab priors for Bayesian equation discovery of nonlinear dynamical systems via sparse linear regression, Mechanical Systems and Signal Processing 161 (2021) 107986. doi:10.1016/j.ymssp.2021.107986. URL <http://dx.doi.org/10.1016/j.ymssp.2021.107986>
- [17] C. Schlosser, M. Korda, Sparse decompositions of nonlinear dynamical systems and applications to moment-sum-of-squares relaxations (2024). arXiv:2012.05572. URL <https://arxiv.org/abs/2012.05572>
- [18] C. M. Bishop, N. M. Nasrabadi, Pattern recognition and machine learning, Vol. 4, Springer, 2006.
- [19] A. P. Dempster, N. M. Laird, D. B. Rubin, Maximum likelihood from incomplete data via the EM algorithm, Journal of the royal statistical society: series B (methodological) 39 (1) (1977) 1–22.

[20] M. I. Jordan, Z. Ghahramani, T. S. Jaakkola, L. K. Saul, An introduction to variational methods for graphical models, *Machine learning* 37 (2) (1999) 183–233.

[21] E. Nuutila, E. Soisalon-Soininen, On finding the strongly connected components in a directed graph, *Information processing letters* 49 (1) (1994) 9–14.

[22] H. Ishwaran, J. S. Rao, Spike and slab variable selection: Frequentist and Bayesian strategies, *The Annals of Statistics* 33 (2) (2005) 730–773. [doi:10.1214/009053604000001147](https://doi.org/10.1214/009053604000001147).

[23] Y. Saad, *Iterative methods for sparse linear systems*, SIAM, 2003.

[24] B. A. Vu, D. Gunawan, A. Zammit-Mangion, R-vgal: a sequential variational Bayes algorithm for generalised linear mixed models, *Statistics and Computing* 34 (3) (Apr. 2024). [doi:10.1007/s11222-024-10422-8](https://doi.org/10.1007/s11222-024-10422-8). URL <http://dx.doi.org/10.1007/s11222-024-10422-8>

[25] J. L. Spouge, Computation of the gamma, digamma, and trigamma functions, *SIAM Journal on Numerical Analysis* 31 (3) (1994) 931–944.

[26] S. E. Özcan, M. M. Ankarali, Sparse Bayesian learning for Koopman based system identification, in: 2025 11th International Conference on Control, Decision and Information Technologies (CoDIT), IEEE, 2025.

[27] E. N. Lorenz, Deterministic nonperiodic flow, *Journal of the Atmospheric Sciences* 20 (1963) 130–141. URL <https://api.semanticscholar.org/CorpusID:15359559>

[28] S. Atasoy, O. K. Karagöz, M. M. Ankarali, Trajectory-free motion planning of an unmanned surface vehicle based on MPC and sparse neighborhood graph, *IEEE Access* 11 (2023) 47690–47700. [doi:10.1109/ACCESS.2023.3275433](https://doi.org/10.1109/ACCESS.2023.3275433).

[29] J. Schoukens, J. Suykens, L. Ljung, Wiener–Hammerstein benchmark, in: Proceedings of the 15th IFAC Symposium on System Identification (SYSID 2009), St. Malo, France, 2009, july 6–8, 2009.